Article

Structure and Function of GDP-Mannose-3‘,5‘-Epimerase: An Enzyme which Performs Three Chemical Reactions at the Same Active Site

Louise L. Major, Beata A. Wolucka, and James H. Naismith

J. Am. Chem. Soc., **2005**, 127 (51), 18309-18320• DOI: 10.1021/ja056490i • Publication Date (Web): 03 December 2005

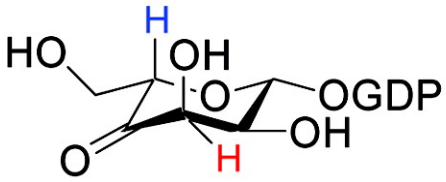

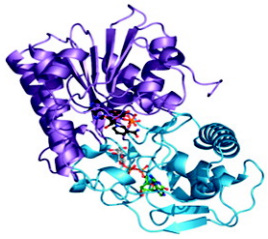

More About This Article

Additional resources and features associated with this article are available within the HTML version:

- Supporting Information
- Links to the 6 articles that cite this article, as of the time of this article download
- Access to high resolution figures
- Links to articles and content related to this article
- Copyright permission to reproduce figures and/or text from this article

View the Full Text HTML

J|A|C|S
ARTICLES
Published on Web 12/03/2005

Structure and Function of GDP-Mannose-3′,5′-Epimerase: An Enzyme which Performs Three Chemical Reactions at the Same Active Site

Louise L. Major,[†] Beata A. Wolucka,[‡] and James H. Naismith*,[†]

Contribution from the Centre for Biomolecular Sciences, University of St. Andrews, North Haugh, St. Andrews, Fife, Scotland KY16 9ST, United Kingdom, and Laboratory of Mycobacterial Biochemistry, Pasteur Institute of Brussels, 642 Engeland Street, 1180 Brussels, Belgium

Received September 21, 2005; E-mail: naismith@st-andrews.ac.uk

Abstract: GDP-mannose-3′,5′-epimerase (GME) from *Arabidopsis thaliana* catalyzes the epimerization of both the 3′ and 5′ positions of GDP-α-D-mannose to yield GDP-β-L-galactose. Production of the C5′ epimer of GDP-α-D-mannose, GDP-β-L-gulose, has also been reported. The reaction occurs as part of vitamin C biosynthesis in plants. We have determined structures of complexes of GME with GDP-α-D-mannose, GDP-β-L-galactose, and a mixture of GDP-β-L-gulose with GDP-β-L-4-keto-gulose to resolutions varying from 2.0 to 1.4 Å. The enzyme has the classical extended short-chain dehydratase/reductase (SDR) fold. We have confirmed that GME establishes an equilibrium between two products, GDP-β-L-galactose and GDP-β-L-gulose. The reaction proceeds by C4′ oxidation of GDP-α-D-mannose followed by epimerization of the C5′ position to give GDP-β-L-4-keto-gulose. This intermediate is either reduced to give GDP-β-L-gulose or the C3′ position is epimerized to give GDP-β-L-4-keto-galactose, then C4′ is reduced to GDP-β-L-galactose. The combination of oxidation, epimerization, and reduction in a single active site is unusual. Structural analysis coupled to site-directed mutagenesis suggests C145 and K217 as the acid/base pair responsible for both epimerizations. On the basis of the structure of the GDP-β-L-gulose/GDP-β-L-4-keto-gulose co-complex, we predict that a ring flip occurs during the first epimerization and that a boat intermediate is likely for the second epimerization. Comparison of GME with other SDR enzymes known to abstract a protein α to the keto function of a carbohydrate identifies key common features.

Introduction

Vitamin C (L-ascorbic acid, L-*threo*-hex-2-enono-1,4-lactone) is a major carbohydrate of plants and an essential micronutrient for animals. In plants, vitamin C has roles in a wide range of processes, including antioxidant defense, photosynthesis, cell division, and growth regulation.[1−3] Additionally, vitamin C is a cofactor for enzymes, including hydroxylases and dioxygenases.[4,5] Leaf ascorbic acid level affects expression of genes involved in defense and hormone signaling pathways.[6] Additionally, plant vitamin C is the major source of dietary vitamin C for humans.

Despite its importance, our understanding of plant vitamin C biosynthesis remains incomplete. Several pathways of vitamin C biosynthesis have been proposed: from D-glucose via D-mannose and L-galactose;[7] from myo-inositol;[8] from galacturonic acid;[9−11] and from L-gulose.[12] It is unclear whether these are independent pathways or whether they interlink, possibly via enzymes with nonspecific activity.[13]

The D-mannose/L-galactose pathway[7,12] (Figure 1) has been refined, with the characterization of most of the enzymes from this pathway: GDP-mannose pyrophosphorylase;[14] GDP-mannose epimerase (GME);[7] L-galactose-1-phosphate phosphatase;[13] L-galactose dehydrogenase;[7,15] L-galactono-1,4-lactone dehydrogenase.[16−18] GDP-L-galactose pyrophosphatase activity has been detected in courgette vascular exudates,[19] and L-gulono-1,4-

[†] University of St. Andrews.
[‡] Pasteur Institute of Brussels.

(1) Noctor, G.; Foyer, C. H. *Annu. Rev. Plant Physiol. Plant Mol. Biol.* **1998**, *49*, 249−279.
(2) Smirnoff, N. *Ann. Bot.* **1996**, *78*, 661−669.
(3) Smirnoff, N. *Curr. Opin. Plant Biol.* **2000**, *3*, 229−235.
(4) Loewus, F. A.; Loewus, M. W. *CRC Crit. Rev. Plant Sci.* **1987**, *5*, 101−119.
(5) Arrigoni, O.; De Tullio, M. C. *Biochim. Biophys. Acta* **2002**, *1569*, 1−9.
(6) Pastori, G. M.; Kiddle, G.; Antoniw, J.; Bernard, S.; Veljovic-Jovanovic, S.; Verrier, P. J.; Noctor, G.; Foyer, C. H. *Plant Cell* **2003**, *15*, 939−951.
(7) Wheeler, G. L.; Jones, M. A.; Smirnoff, N. *Nature* **1998**, *393*, 365−369.
(8) Lorence, A.; Chevone, B. I.; Mendes, P.; Nessler, C. L. *Plant Physiol.* **2004**, *134*, 1200−1205.
(9) Loewus, F. A.; Kelly, S. *Arch. Biochem. Biophys.* **1961**, *95*, 483−493.
(10) Agius, F.; González-Lamothe, R.; Caballero, J. L.; Muñoz-Blanco, J.; Botella, M. A.; Valpuesta, V. *Nat. Biotechnol.* **2003**, *21*, 177−181.
(11) Isherwood, F. A.; Mapson, L. W. *Biochem. J.* **1956**, *64*, 13−22.
(12) Wolucka, B. A.; van Montagu, M. *J. Biol. Chem.* **2003**, *278*, 47483−47490.
(13) Laing, W. A.; Bulley, S.; Wright, M.; Cooney, J.; Jensen, D.; Barraclough, D.; MacRae, E. *Proc. Natl. Acad. Sci. U.S.A.* **2004**, *101*, 16976−16981.
(14) Conklin, P. L.; Norris, S. R.; Wheeler, G. L.; Williams, E. H.; Smirnoff, N.; Last, R. L. *Proc. Natl. Acad. Sci. U.S.A.* **1999**, *96*, 4198−4203.
(15) Gatzek, S.; Wheeler, G. L.; Smirnoff, N. *Plant J.* **2002**, *30*, 541−553.
(16) Oba, K.; Fukui, M.; Imai, Y.; Iriyama, S.; Nogami, K. *Plant Cell Physiol.* **1994**, *35*, 473−478.
(17) Ostergaard, J.; Persiau, G.; Davey, M. W.; Bauw, G.; van Montagu, M. *J. Biol. Chem.* **1997**, *272*, 30009−30016.
(18) Imai, T.; Karita, S.; Shiratori, G.; Hattori, M.; Nunome, T.; Oba, K.; Hirai, M. *Plant Cell Physiol.* **1998**, *39*, 1350−1358.
(19) Hancock, R. D.; McRae, D.; Haupt, S.; Viola, R. *BMC Plant Biol.* **2003**, *3*, 7.

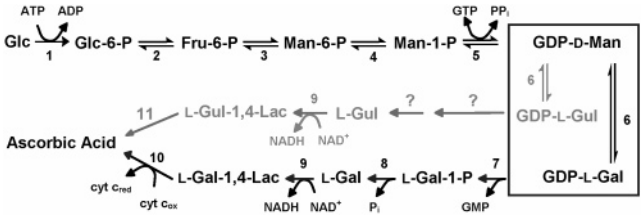

Figure 1. Proposed de novo biosynthetic pathway of ascorbic acid in plants. The D-mannose/L-galactose pathway (7) is in black, and the proposed L-gulose pathway (20) is in gray. The reactions catalyzed by GDP-mannose epimerase (GME) are boxed. Enzymes: **1**, hexokinase; **2**, phosphoglucose isomerase; **3**, phosphomannose isomerase; **4**, phosphomannose mutase; **5**, GDP-mannose pyrophosphorylase; **6**, GME; **7**, putative GDP-L-galactose pyrophosphatase; **8**, L-galactose-1-phosphate phosphatase; **9**, L-galactose dehydrogenase; **10**, L-galactono-1,4-lactone dehydrogenase; **11**, L-gulono-1,4-lactone dehydrogenase. Abbreviations: Glc, D-glucose; Fru, D-fructose; Man, D-mannose; L-Gal, L-galactose; L-Gal-1,4-Lac, L-galactono-1,4-lactone; L-Gul, L-gulose; L-Gul-1,4-Lac, L-gulono-1,4-lactone.

lactone dehydrogenase activity has been detected in the mitochondrial[16] and cytosolic[12] fractions of potato tubers. The *Arabidopsis thaliana* (*A. thaliana*) gene for GME has been cloned and the protein expressed in *Escherichia coli* (*E. coli*).[20] GME is a late methyl-jasmonate responsive gene involved in stress responses of plants.[21] Sequence analysis showed that GME is a member of the extended short-chain dehydratase/reductase (SDR) family, although with a modified glycine-rich nucleotide binding motif[22] (GAGGFIA instead of GXXGXXG).[23] GME epimerizes the C3′ and C5′ positions of GDP-α-D-mannose to give GDP-*β*-L-galactose. Reversible epimerization of GDP-α-D-mannose to GDP-*β*-L-galactose had previously been observed in extracts from the green algae *Chlorella pyrenoidosa*.[24,25] Tritium-labeling studies showed that the epimerized protons are exchanged with solvent.[26] Recently, GME has been reported to produce GDP-*β*-L-gulose in addition to GDP-*β*-L-galactose; this second product has been proposed to be a precursor of vitamin C in plants[12] (Figure 1). Epimerization of carbon atoms, such as C3′ and C5′, in GDP-α-D-mannose via a direct deprotonation is chemically impossible for enzymes; the pK_a for these protons would be well over 30. Modification of the sugar ring, to lower the pK_a of these protons, is required prior to epimerization.

GME is a member of the SDR class of enzymes, a diverse group with substrates ranging from steroids and alcohols to aromatic compounds. While typical SDR enzymes have around 250 residues, the extended SDR enzymes, such as GME, have around 350 residues.[27] Extended SDR enzymes catalyze oxidation, dehydration, decarboxylation, reduction, epimerization, and isomerization reactions. The key feature of the SDR superfamily is the transfer of a hydride between substrate and enzyme-bound NAD(P)$^+$ cofactor. Assuming hydride transfer, a chemically reasonable mechanism can be predicted for GME (Scheme 1). The C4′ atom is oxidized by GME-NAD$^+$ to give a keto sugar

Scheme 1. Reactions Catalyzed by GME (R= OGDP)

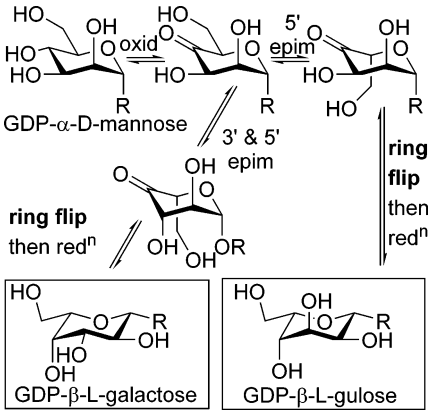

Scheme 2. Reaction Catalyzed by GMER (R= OGDP)

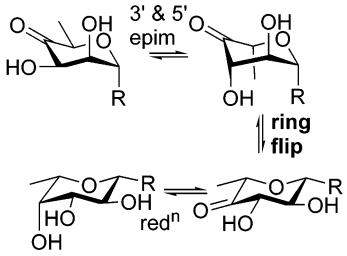

and GME-NADH. The protons attached to C3′ and C5′ are now α to a keto function, and their pK_a drops to around 18[28] (Scheme 1). These protons are epimerized by removal from one face and replacement on the opposite face, inverting the chirality at the carbon center. Finally, the C4′ keto group is reduced by GME-NADH to give the product and GME-NAD$^+$ (Scheme 1). Thus, GME could more correctly be termed GDP-mannose-4′-oxidase/3′,5′-epimerase/4′-reductase, reflecting its ability to catalyze three distinct chemical reactions. During epimerization, the carbohydrate changes from an axial configuration of the nucleotide to an equatorial configuration. This is a consequence of a ring flip which must occur during epimerization (Scheme 1).

The efficiency of GME in combining chemical reactions is unusual, given that in other sugar nucleotide pathways an equivalent series of reactions requires multiple enzymes. For example, in bacterial L-rhamnose synthesis, three enzymes, RmlB (oxidation), RmlC (epimerization), and RmlD (reduction), carry out each of the chemical reactions in turn.[29] In addition to oxidation of the hydroxyl at C4′, RmlB also dehydrates C6′. Other SDR enzymes are known to combine epimerization with redox chemistry, for example, GDP-4-keto-6-deoxy-D-mannose-3,5-epimerase-4-reductase (GMER) (also known as GDP-fucose synthetase) from the GDP-fucose biosynthetic pathway. GMER epimerizes the C3′ and C5′ positions of GDP-4-keto-6-deoxy-mannose then reduces the C4′-ketone[30] (Scheme 2). Inhibition of the biosynthesis of GDP-fucose is appealing in the treatment of inflammatory diseases and bacterial infection.[31] GMER shares 24% identity with GME and has been probed by several studies, including site-directed mutagenesis and structural descriptions

(20) Wolucka, B. A.; Persiau, G.; van Doorsselaere, J.; Davey, M. W.; Demol, H.; Vandekerckhove, J.; van Montagu, M.; Zabeau, M.; Boerjan, W. *Proc. Natl. Acad. Sci. U.S.A.* **2001**, *98*, 14843−14848.
(21) Wolucka, B. A.; Goossens, A.; Inzé, D. *J. Exp. Bot.* **2005**, *56*, 2527−2538.
(22) Wierenga, R. K.; De Maeyer, M. C. H.; Hol, W. G. J. *Biochemistry* **1985**, *24*, 1346−1357.
(23) Persson, B.; Kallberg, Y.; Oppermann, U.; Jörnvall, H. *Chem.-Biol. Interact.* **2003**, *143*−*144*, 271−278.
(24) Barber, G. A. *Arch. Biochem. Biophys.* **1971**, *147*, 619−623.
(25) Hebda, P. A.; Behrman, E. J.; Barber, G. A. *Arch. Biochem. Biophys.* **1979**, *194*, 496−502.
(26) Barber, G. A. *J. Biol. Chem.* **1979**, *254*, 7600−7603.
(27) Jörnvall, H.; Persson, B.; Krook, M.; Atrian, S.; Gonzàlez-Duarte, R.; Jeffery, J.; Ghosh, D. *Biochemistry* **1995**, *34*, 6003−6013.
(28) Richard, J. P.; Amyes, T. L. *Curr. Opin. Chem. Biol.* **2001**, *5*, 626−633.
(29) Giraud, M.-F.; Naismith, J. H. *Curr. Opin. Struct. Biol.* **2000**, *10*, 687−696.
(30) Chang, S.; Duerr, B.; Serif, G. *J. Biol. Chem.* **1988**, *263*, 1693−1697.
(31) Menon, S.; Stahl, M. L.; Kumar, R.; Xu, G.-Y.; Sullivan, F. X. *J. Biol. Chem.* **1999**, *274*, 26743−26750.

Table 1. Summary of Data Collection and Refinement Statistics

	GME K178R			Wt-GME	GME Y174F	GME K217A
	native	SeMet		native	native	native
incubated with				GDP-D-mannose	GDP-L-galactose	GDP-D-mannose
		peak	remote			
wavelength (Å)	0.9340	0.97908	0.88570	1.54180	0.93300	0.93300
space group	$P2_1$	$P2_1$	$P2_1$	$P2_1$	$P2_1$	$P2_1$
cell dimensions (Å)	$a = 62.3$	$a = 62.85$		$a = 62.8$	$a = 62.5$	$a = 62.5$
	$b = 82.5$	$b = 83.54$		$b = 83.8$	$b = 83.3$	$b = 83.2$
	$c = 65.9$	$c = 66.0$		$c = 66.2$	$c = 66.1$	$c = 66.2$
cell dimension (deg)	$\beta = 98.8$	$\beta = 98.7$		$\beta = 98.9$	$\beta = 98.9$	$\beta = 99.0$
resolution (Å)	1.5	2.0	2.0	2.0	1.4	1.7
unique reflections	105071	44663	44831	45789	126826	73777
redundancy	3.7 (3.6)	5.8 (5.5)	3.2 (3.2)	3.6 (3.5)	3.6 (3.5)	3.8 (3.8)
completeness (%)	99.9 (99.9)	98.0 (95.6)	98.1 (97.5)	99.6 (97.7)	96.7 (95.4)	99.8 (99.7)
R_{merge} (%)	4.8 (20.6)	7.3 (24.2)	5.5 (15.4)	8.5 (45.1)	5.4 (22.8)	9.3 (44.5)
I/σ	9.6 (3.6)	8.9 (3.1)	7.5 (4.6)	7.9 (1.7)	17.9 (5.5)	13.2 (2.2)
No. of non-H atoms	7221			7003	7235	6970
R_{factor} (%)	11.5			14.6	10.3	12.7
R_{free} (5% of data) (%)	16.6			21.9	14.0	19.2
rms deviations						
bond lengths (Å)	0.021			0.020	0.020	0.021
bond angles (deg)	1.978			1.828	1.984	1.839
Mean B value (Å^2)	11			23	9	16
rmsd of subunit A vs B (Å) measured for core region	0.241			0.239	0.253	0.224
PDB accession number	2c54			2c59	2c5a	2c5e

of its complexes with NADPH and NADP$^+$.[32,33] In plants, nucleotide−rhamnose synthase/epimerase−reductase combines RmlC and RmlD activity.[34] Epimerization can be separated into two crude chemical categories. One is direct oxidation and reduction at the carbon center with concomitant inversion.[35] This is exemplified by UDP-galactose 4-epimerase (GalE), which has been extensively studied by structural techniques.[36,37] The other is the epimerization α to an activated function,[38] such as that carried out by GMER,[30] which epimerizes α to a keto function (Scheme 2). No substrate or product complex of an SDR enzyme known to epimerize a carbohydrate α to an activated function has been reported. Therefore, site-directed mutagenesis, enzyme mechanism, and inhibitor studies are guided by models rather than experimental information. Given the complexity of the substrates and the occurrence of ring flips during catalysis, this is a serious limitation in developing a clear understanding of the chemistry.

To probe GME, we constructed a K178R mutant GME; K178 is part of the catalytic triad of SDR enzymes, and in GMER, such a mutation resulted in a 40-fold reduction of activity.[38] By using this "inactivated" GME, we aimed to determine co-complexes. Interestingly, without addition of any substrates or cofactors, the mutant crystallized as a complex containing a mixture of GDP-β-L-4-keto-gulose (Scheme 1) and product GDP-β-L-gulose, as well as a mixture of NAD$^+$ and NADH. On the basis of this structure, we made further mutants and examined their activity by HPLC. We used these mutants to determine co-complexes of GME with GDP-α-D-mannose and GDP-β-L-galactose. We have also determined a native enzyme structure, and this shows a mixture of carbohydrates bound at the active site. Combining these data has allowed us to propose a detailed chemical mechanism for GME.

Results

Overall Structure of GME K178R. We have determined several structures (including mutants and wild type) of GME (Table 1). We discuss the K178R structure as this was the first one we studied. K178R GME was crystallized in the absence of cofactors or substrates and diffracted to 1.5 Å, with cell dimensions of $a = 62.3$ Å, $b = 82.5$ Å, $c = 65.9$ Å, $\beta = 98.8°$, and spacegroup $P2_1$. Molecular replacement attempts failed, and selenomethionine incorporation coupled to multiwavelength anomalous diffraction was used to solve the structure. The GME monomer (Figure 2a) consists of 377 amino acids with a molecular mass of 42 758 Da. GME crystallized as a dimer in the asymmetric unit (Figure 2b). The extreme C- and N-termini of the protein were not observed in the crystal structures (Figure 2a). Initial inspection of the map revealed density for a sugar nucleotide and for NAD$^+$ bound to the enzyme. The structure can be decomposed into the Rossmann fold domain, which binds NAD$^+$ (residues 1−101, 112−143, 161−201, 248−269, 309−322, and 363−375), and the substrate domain, which binds sugar nucleotide (residues 102−111, 144−160, 202−247 and 270−308, and 323−362). The organization of the secondary structure elements within the domains and the relationship between the domains are similar to that described for RmlB.[39] Briefly, GME binds NAD$^+$ in a modified Rossmann fold with seven parallel β-strands in its β-sheet (β3, β2, β1, β4, β5, β7, and β12) flanked

(32) Rizzi, M.; Tonetti, M.; Vigevani, P.; Sturla, L.; Bisso, A.; De Flora, A.; Bordo, D.; Bolognesi, M. *Structure* **1998**, *6*, 1453−1465.
(33) Somers, W. S.; Stahl, M. L.; Sullivan, F. X. *Structure* **1998**, *6*, 1601−1612.
(34) Watt, G.; Loeoff, C.; Harper, A. D.; Bar-Peled, M. *Plant Physiol.* **2004**, *134*, 1337−1346.
(35) Allard, S. T. M.; Giraud, M.-F.; Naismith, J. H. *Cell. Mol. Life Sci.* **2001**, *58*, 1650−1665.
(36) Thoden, J. B.; Frey, P. A.; Holden, H. M. *Biochemistry* **1996**, *35*, 2557−2566.
(37) Thoden, J. B.; Frey, P. A.; Holden, H. M. *Protein Sci.* **1996**, *5*, 2149−2161.
(38) Rosano, C.; Bisso, A.; Izzo, G.; Tonetti, M.; Sturla, L.; De Flora, A.; Bolognesi, M. *J. Mol. Biol.* **2000**, *303*, 77−91.

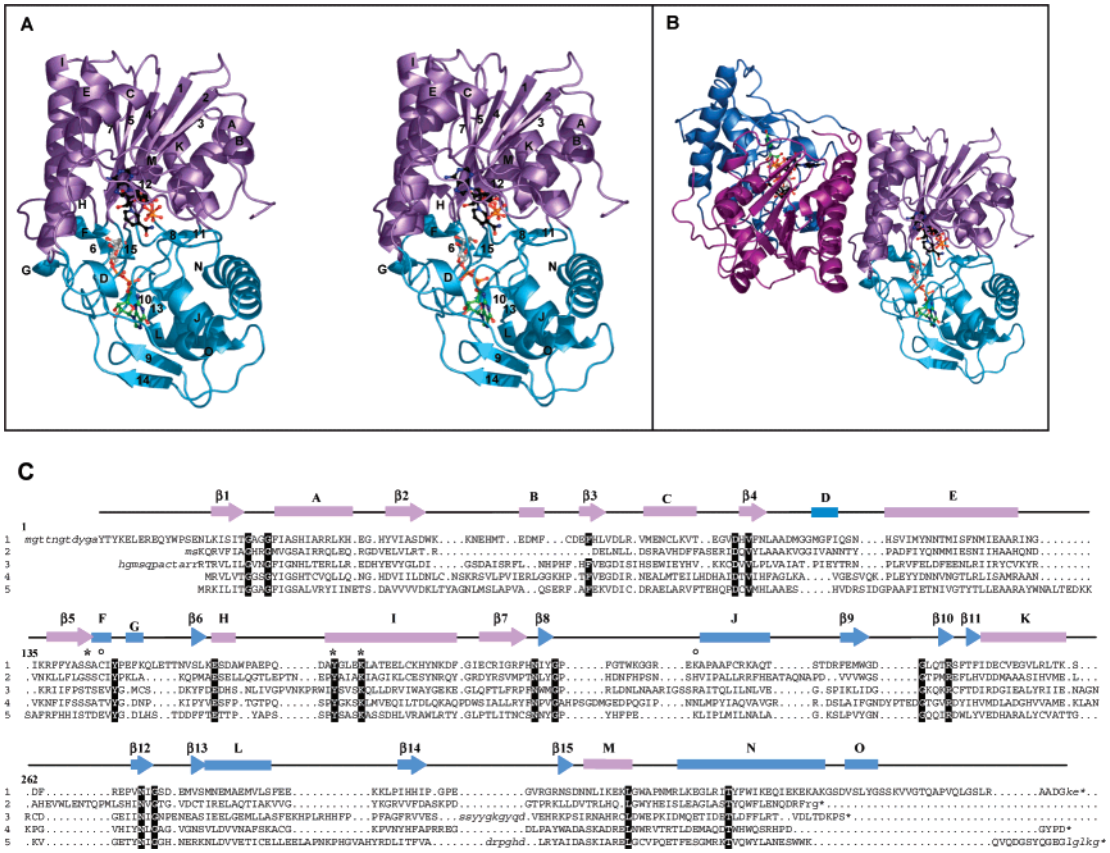

Figure 2. GME structure. (A) stereodiagram of monomer A of Y174F GME. The NAD^+ binding domain is colored lilac, and the substrate binding domain pale blue. Bound NAD^+ and GDP-β-L-galactose molecules are shown. NAD^+ carbon atoms are colored black, GDP carbon atoms green, and galactose carbon atoms gray. In all molecules, oxygen atoms are colored red, nitrogen blue, and phosphorus orange. (B) Cartoon of the GME Y174F dimer. Monomer A is colored as in Figure 2A. In monomer B, the nucleotide binding domains are colored purple, and the ligand binding domain is colored blue. Monomer A has ordered residues 13−375, monomer B ordered residues 12−371. Ligands are shown and colored as in Figure 2A. (C) Structural alignment of GME (sequence 1), with SDR homologues. The homologues are *E. coli* proteins: 2, GMER (1bsv); 3, ArnA decarboxylase domain (2bll); GalE (1xel), and RmlB (1bxk). Identical residues are highlighted, ∗ indicates residues from the SDR catalytic triad, ° marks the GME candidate acid/base residues for epimerization. Helices B, F, G, H, and O are 310 helices. Helix O is only present in GME subunit A. Residues written in lower case italic script were not in the pdb files (disordered regions). The indicated secondary structure is from Y174F GME subunit A and is colored as in Figure 2A.

by three helices on each face (αC, αE, and αI on one face with αA, αB, and αK on the other) (Figure 2a). The Rossmann fold has insertions of additional secondary structure elements after β4 and β5, which contribute to the substrate binding domain. The substrate binding domain is primarily helical with two short parallel β-sheets (β8 and β11, β6 and β15) and an antiparallel β-sheet (β10, β13). Three loops from the GME C-terminal fold up against the Rossmann fold (includes αK, αM, and residues 363−375). Like RmlB, GME is a dimer with helices from one face of the Rossmann fold forming the dimer interface (Figure 2b). A superposition of the two monomers in the asymmetric unit shows that the N-terminus, C-terminus, and four loops differ by up to 2 Å for Cα positions. Although the loops (229−234, 285−295, 314−320, and 342−352) are found in the substrate binding domain, they are involved in crystal packing. The N- and C-termini are simply flexible. Excluding these regions, the root-mean-square deviation (rmsd) for 316 Cα atoms is 0.26 Å. Crystal structures of the protein from the mutants (K217A, K178R, Y174F) and wild type with different sugar nucleotides are isomorphous (Table 1). Differences between monomers within each crystal are greater than differences between the same monomer from different crystals. Thus crystal packing perturbs the protein to a greater extent than either mutation or differences in ligand. Coordinates and experimental data have been deposited with the PDB.

Relationship to Other SDR Enzymes. The closest structural homologues to GME are four *E. coli* proteins: GMER (pdb file 1BSV[33]); ArnA decarboxylase domain (pdb file 2BLL[40]); UDP-galactose 4-epimerase (GalE) (pdb file 1XEL [41]); and RmlB (pdb file 1BXK). These enzymes are all extended SDR family members, and at the heart of their mechanisms is the transfer of hydride. The additional chemistry they catalyze is, however, quite different. GMER catalyzes epimerization at C3′ and C5′ positions before reducing the C4′ keto sugar (Scheme 2). Like GME, GMER must have a requirement for an acid/base pair to catalyze epimerization. Site-directed mutagenesis has suggested residues Cys109 and H179 fill this role in GMER.[38] The ArnA decarboxylase domain (358 residues) catalyses NAD^+ dependent oxidation at C4′ of UDP-glucuronic acid, followed by decarboxylation at the C5′ position, producing UDP-4-keto-arabinose.[40,42,43] The role of Glu434 is unclear but

(39) Allard, S. T. M.; Giraud, M.-F.; Whitfield, C.; Graninger, M.; Messner, P.; Naismith, J. H. *J. Mol. Biol.* **2001**, *307*, 283−295.

(40) Williams, G. J.; Breazeale, S. D.; Raetz, C. R. H.; Naismith, J. H. *J. Biol. Chem.* **2005**, *280*, 23000−23008.

(41) Thoden, J. B.; Frey, P. A.; Holden, H. M. *Biochemistry* **1996**, *35*, 5137−5144.

(42) Gatzeva-Topalova, P. Z.; May, A. P.; Sousa, M. C. *Biochemistry* **2004**, *43*, 13370−13379.

has been suggested to ensure the deprotonation of the carboxylic acid required for decarboxylation. GalE catalyzes epimerization at C4′ of the nucleotide sugar UDP-galactose. In contrast to GMER and GME, the epimerization is achieved via oxidation and reduction at C4′, while the sugar rotates at the active site.[44] No acid/base pair is required for this process. RmlB catalyzes C4′ oxidation, then Glu136, acting as the base, extracts a C5′ proton. Asp135 protonates the 6OH group, which is then eliminated as water. The glucosene intermediate is then reduced to give the product.[45−47]

There are only 17 absolutely conserved residues in the structural alignment of these four proteins. Two of these are the catalytic triad tyrosine (GME Y174) and lysine (GME K178) residues; the third residue is found as both Ser and Thr. In the main, conserved residues are either concerned with ligand binding or play a structural role. In GME, N203 is located at the substrate binding domain, and its side chain hydrogen bonds with the phosphate groups of GDP and to water molecules. In GalE, this residue fulfills a similar role. We therefore identify this residue as important for substrate recognition. This may be in addition to or in place of its role in maintaining correct folding for SDR enzymes.[48]

NAD^+ Binding Site. NAD^+ is found in all our crystal structures (with no exogenous addition), and enzyme activity is not increased by its addition, suggesting NAD^+ is tightly bound by the enzyme. NAD^+ is located in the N-terminal domain of protein and is bound by 12 direct hydrogen bonds, 10 bridging water molecules, and hydrophobic interactions (Figure 3a). The side chains of K178, Y174, D78, and D58 directly interact with NAD^+ and are conserved in other NAD^+ binding extended SDR enzymes. GMER binds $NADP^+$, and there are some small differences in the details of interaction resulting from the additional phosphate. In the GME complexes, NAD^+ is found in the syn-conformation with a hydrogen bond between the nucleotide phosphate and nicotine amide. The presence of this hydrogen bond has been identified as crucial in regulation of the redox potential of the NAD^+/NADH couple in an extended SDR enzyme.[49] In GME, the adenine ring binds close to the GAGGFIA (Wierenga[22]) motif in the loop between β1 and αA. The GAGGFIA sequence is unusual, and in extended SDRs, GxxGxxG is normally found.[23] The additional CH_3 group does not change the conformation of the backbone but appears to fit into a small hydrophobic void, perhaps decreasing enzyme flexibility. Two residues, G34 and A40, from the Wierenga motif make hydrogen bonds to NAD^+ through a bridging water molecule. This water has been observed in around 70% of Rossmann fold structures.[50]

Co-complexes and GDP Binding Site. We determined the structure of K178R GME without any exogenous cofactors or substrates. Different electron density was clearly apparent for a GDP molecule linked at the equatorial position to an L-configured carbohydrate ring. The high resolution (1.5 Å) of the study allowed us to unambiguously identify this sugar as GDP-β-L-gulose (Figure 3b). We have confirmed by HPLC analysis of the crystals that there is no significant amount of GDP-α-D-mannose or GDP-β-L-galactose present. There is one major component with the mass predicted for GDP-gulose (Figure 4a). From the electron density, it is clear that there is a second molecule present, and on the basis of the density at C4′, we interpret this as GDP-β-L-4-keto-gulose (Figure 3b). Both GDP-sugars must therefore have co-purified with the mutant enzyme. The electron density shows that NAD is found as mixture of flat NAD^+ and buckled NADH (Supporting Information Figure S4). We postulate that this is a result of an equilibrium, peculiar to the crystalline state, between GDP-β-L-gulose and NAD^+ on one side with GDP-β-L-4-keto-gulose and NADH on the other. We assume that, upon dissolution of the crystals for HPLC analysis, GDP-L-4-keto-gulose is reduced to GDP-β-L-gulose. Incubating wild-type GME with GDP-α-D-mannose shows clearly that NAD^+ and GDP-linked carbohydrate are bound. HPLC analysis of protein incubated with GDP-α-D-mannose shows the presence of GDP-α-D-mannose, GDP-β-L-galactose, and GDP-β-L-gulose in the ratio 0.8:0.15:0.05 (Figure 4b). Given the limited resolution (2.0 Å), we conservatively fitted the electron density as a mixture of GDP-α-D-mannose and GDP-β-L-galactose (Supporting Information Figure S7). To obtain an authentic substrate complex, we incubated K217A GME with GDP-α-D-mannose prior to and during crystallization. The resulting complex diffracted to 1.7 Å, and both electron density analysis (Supporting Information Figure S8) and HPLC analysis confirmed only GDP-α-D-mannose was present in solution. Using a similar philosophy, we incubated the largely inactive Y174F GME mutant with GDP-β-L-galactose prior to and during crystallization. The resulting complex diffracted to 1.4 Å, and both electron density analysis (Supporting Information, Figure S9) and HPLC analysis confirmed only GDP-β-L-galactose was present in solution. In total, there are eight monomers of GME, including protein mutants, substrate, product, and intermediate complexes. Superposition of the complexes reveals that the GDP moiety is bound identically in all structures. M105, A218, E216, N203, K225, S356, Q241, and R243 all make direct hydrogen bonds with the GDP (Figure 3c); two of these residues (R243 and N203) are conserved in GMER, RmlB, GalE, and the ArnA decarboxylase domain. The guanosine ring is sandwiched between the side chains of F222 and W236, with which it forms a π stacking interaction. In addition, there are a number of van der Waals contacts with G104, M277, A221, and M235 (Figure 3c). K225 superimposes on R187 of GMER, which was shown to be important in substrate binding;[38] in GME, K225 forms a hydrogen bond with the guanosine hydroxyl.

Carbohydrate Binding Site. The carbohydrate rings are bound in a pocket adjacent to the nicotinamide of NAD^+. GDP-α-D-mannose is found in both native and K217A structures. The positions of the ring are slightly different (0.8 Å for C4′), and this may be a result of the absence of the side chain of K217, which changes the packing considerations at the active site. In structures (native and Y174F) containing GDP-β-L-galactose, the carbohydrate atom positions differ by 0.1−0.7 Å. The atoms of GDP-β-L-gulose and GDP-β-L-4-keto-gulose are close (0.1−

(43) Gatzeva-Topalova, P. Z.; May, A. P.; Sousa, M. C. *Structure* **2005**, *13*, 929−942.
(44) Thoden, J. B.; Holden, H. M. *Biochemistry* **1998**, *37*, 11469−11477.
(45) Gross, J. W.; Hegeman, A. D.; Vestling, M. M.; Frey, P. A. *Biochemistry* **2000**, *39*, 13633−13640.
(46) Gross, J. W.; Hegeman, A. D.; Gerratana, B.; Frey, P. A. *Biochemistry* **2001**, *40*, 12497−12504.
(47) Hegeman, A. D.; Gross, J. W.; Frey, P. A. *Biochemistry* **2002**, *41*.
(48) Filling, C.; Nordling, E.; Benach, J.; Berndt, K. D.; Ladenstein, R.; Jörnvall, H.; Oppermann, U. *Biochem. Biophys. Res. Commun.* **2001**, *289*, 712−717.
(49) Beis, K.; Allard, S. T. M.; Hegeman, A. D.; Murshudov, G.; Philp, D.; Naismith, J. H. *J. Am. Chem. Soc.* **2003**, *125*, 11872−11878.
(50) Bottoms, C. A.; Smith, P. E.; Tanner, J. J. *Protein Sci.* **2002**, *11*, 2125−2137.

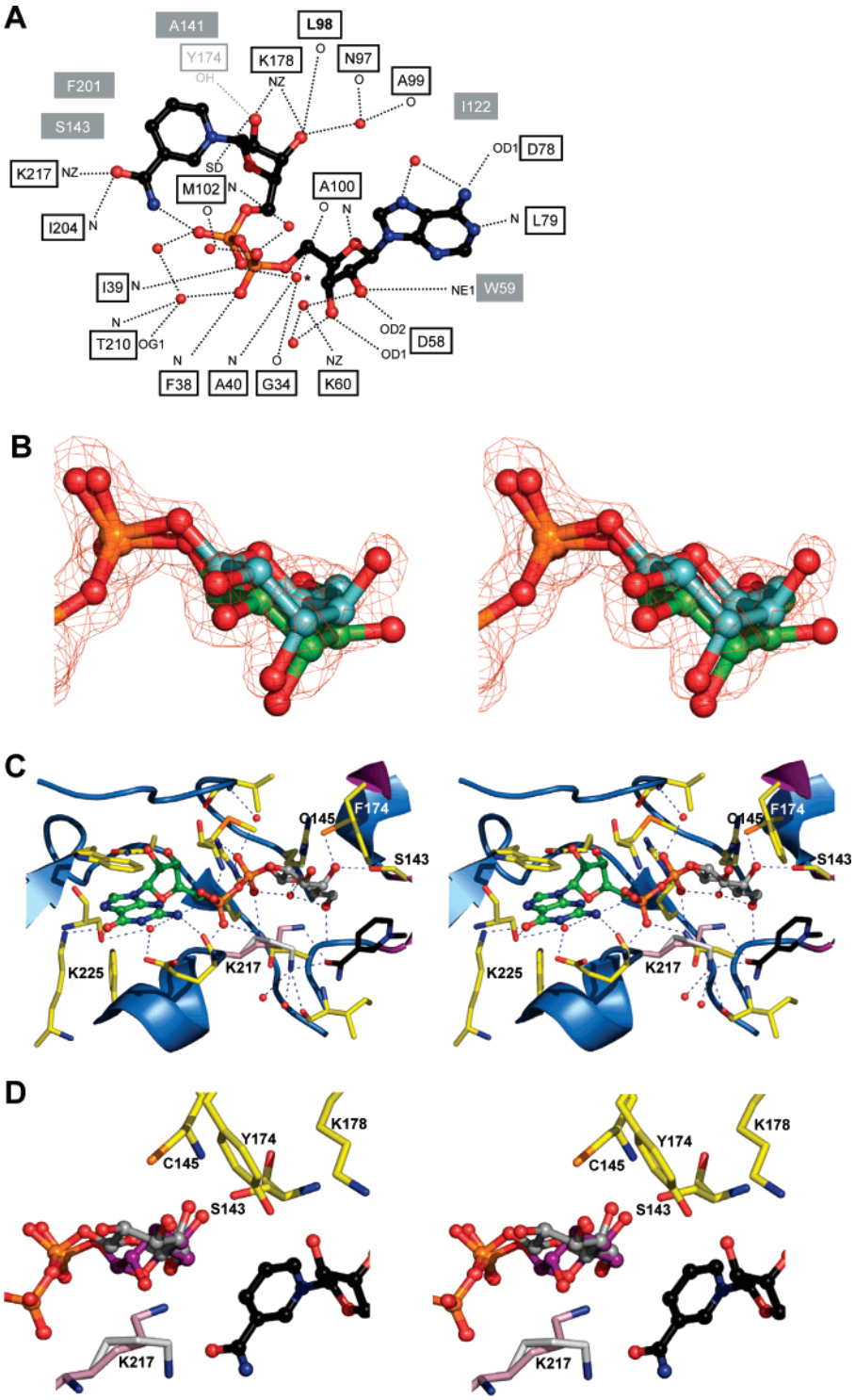

Figure 3. Ligand binding to GME. (A) Schematic of NAD^+ binding to GME in the Y174F GME mutant, the highest resolution structure. Hydrophobic interactions include π stacking by W59. Distances and interactions were determined by Ligplot.[51] Gray boxes indicate residues with hydrophobic interactions to the ligand. Dotted lines represent hydrogen bonds. The Y174 interaction, observed in the K217A, K178R, and wt structures, is added to this figure for completeness. The aromatic ring of F174 in the Y174F mutant structure is unchanged in position or orientation from the aromatic ring of Y174 in the other structures. The water with an asterisk beside it has been observed in >70% of all SDR enzyme structures.[50] Atom color is as in Figure 2A. (B) Stereodiagram of gulose/4-keto-gulose unbiased $F_o - F_c$ density observed in the ligand binding pocket of K178R GME. Electron density is shown as a chickenwire representation contoured at 2.5σ. The final refined positions of the GDP-L-β-gulose and GDP-L-β-4-keto-gulose are shown. Gulose carbons are green, 4-keto-gulose carbons are pale blue. Other atoms are colored as in Figure 2A. (C) Stereodiagram of GDP-galactose bound to Y174F GME, hydrogen bonds are shown as dashed lines. The two conformations of K217 are indicated with pink or white carbon atoms. For the remainder of the protein, carbon atoms are colored yellow. All other atoms are colored as in Figure 2A. Water molecules are shown as red spheres. (D) Superposition of mannose and galactose from Y174F galactose and K217A mannose structures, with catalytic residues. Mannose carbons are colored purple, and all other atoms are colored as in Figure 3C. The two conformations of K217 from the Y174F structure are shown. The position of Y174 is shown as located by the K217A structure for clarity.

0.7 Å) to those of GDP-β-L-galactose, with the exception of O3′, which has a different configuration. The GDP-β-L-4-keto-gulose refines to a slightly different position (0.75 Å for C3′ atoms) relative to GDP-β-L-gulose (both in K178R).

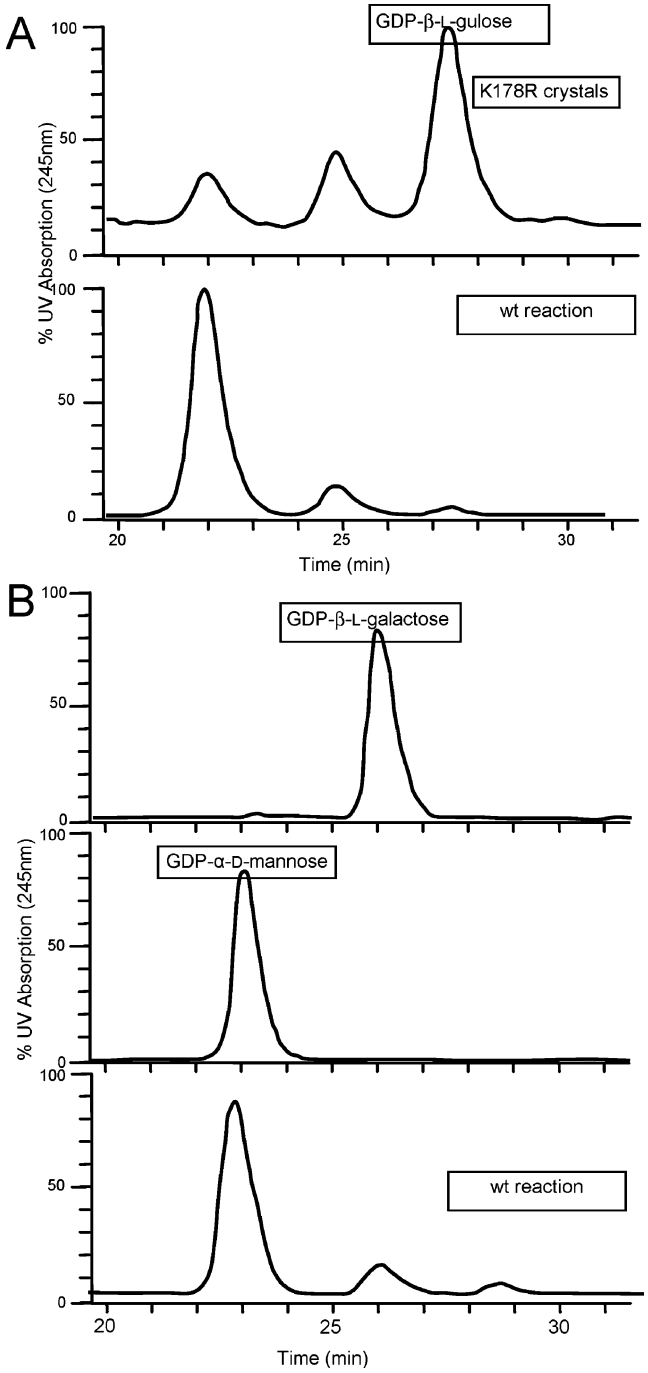

Figure 4. Identification of the three sugar nucleotides made by GME. (A) The top panel shows the nucleotide sugars extracted from K178R, the crystal structure identifies GDP-L-β-gulose as the major sugar nucleotide in the crystal. The lower panel shows the wild-type reaction with its three characteristic peaks. (B) The top panel shows the trace of authentic GDP-β-L-galactose, the middle panel authentic GDP-α-D-mannose, and the lower panel the normal wild-type reaction with its three peaks.

Superimposing GDP-β-L-galactose and GDP-α-D-mannose complexes reveals that, despite the ring flip and double epimerization, C5′, C6′, O6′, C4′, C3′, and O3′ atoms of the carbohydrate overlap (Figure 3d). O6′ hydrogen bonds to the backbone amide of N203 and to a water molecule, which bridges to the β-phosphate of GDP. O4′ is hydrogen bonded to C145 and Y174; O3′ is hydrogen bonded to G103. C5′ and C3′ are within 4 Å of C145, and C4′ ranges 3.8−4.1 Å from C4 of the nicotinamide ring (Figure 3d). O5′, C1′, O1′, C2′, and O2′ atoms do not overlap, and we have split the discussion of those interactions into the GDP-α-D-mannose and the GDP-β-L-galactose complexes. In the GDP-α-D-mannose complex, O5′ hydrogen bonds to the same bridging water as O6′, while O2′ makes a hydrogen bond with the carbonyl backbone of G103. In GDP-β-L-galactose, O5′ in addition to the hydrogen bond through the same bridging water (described above) makes a hydrogen bond to R306. O2′ and O1′ atoms make no hydrogen bonds in GDP-β-L-galactose. Comparing GDP-β-L-gulose with GDP-β-L-galactose complexes shows they have the same interactions with protein, except O3′, which differs in conformation between the compounds. In GDP-β-L-gulose, the axial O3′, although close to the carbonyl of G103, no longer has the optimal angle for a hydrogen bond. In all six monomers with K217 at the active site, the side chain exhibits multiple conformations. The strongest density for the side chain always shows the NZ atom hydrogen bonding to the amide of nicotinamide above the sugar ring (Figure 3d). The separation between the NZ atom and C3′ and C5′ position ranges from 5.2 to 6.5 Å. In the B monomer of the GDP-β-L-galactose structure, a second conformer is quite clearly seen, although the density is weak for the NZ atom (Supporting Information Figure S13). This conformation is also present in monomer A and in other structures, but the density is even weaker and cannot be fitted. In this second position, the NZ atom sits above the plane of the ring and is 2.9 Å from C3′ and 2.7 Å from C5′ (Figure 3c).

Biochemical Characterization. When GME is incubated with GDP-α-D-mannose, three GDP-sugar peaks were observed after ion-pair reversed-phase HPLC (Figure 4). GDP-α-D-mannose (80%) and GDP-β-L-galactose (15%) peaks were confirmed by spiking with standards. The GDP-β-L-gulose peak (5%) was confirmed by coelution with the major peak from K178R GME crystals (which had been verified by crystallography as GDP-β-L-gulose). Coupled HPLC−MS in negative ion mode showed that the major constituent of each of these three peaks has a mass of 604, which is consistent with their chemical formula. No other peaks with a mass of 604 were identified, suggesting that GDP-D-altrose is not produced by GME in significant amounts. It is possible that GDP-D-altrose coelutes with the other sugars. Increasing the amount of protein and time of incubation did not alter the ratios of sugars. We have also incubated the enzyme with each of GDP-β-L-galactose and GDP-β-L-gulose and find the same equilibrium. GME therefore catalyzes the interconversion of the three sugars, and their proportions are determined by the thermodynamic equilibrium. These data confirm the earlier report that both GDP-β-L-gulose and GDP-β-L-galactose are made by the enzyme.[12] It also suggests that in *A. thaliana* a pool of both of these sugars exists for their downstream pathways. The flux through the pathway of course would then be regulated by coupling to downstream enzymes, which consume one sugar in preference to another.

Using the HPLC assay, K217A, C145A, and Y174F were found to be inactive even with high concentrations of enzymes with prolonged incubation times (Table 2 and Supporting Information Figure S14). K178R, R306A, and C145S did show some activity at higher enzyme concentrations, suggesting some residual activity for these mutations. The inactivity or severely impaired activity of K178R and Y174F GME is not surprising

Table 2. Relative Amounts of Products Observed from GDP-α-D-Mannose[a]

enzyme	μM	% M	% Ga	% Gu
GME	0.3	80.3 ± 1.7	15.4 ± 0.9	4.2 ± 0.8
C145S	0.3	99.7 ± 0.2	0.2 ± 0.1	0.1 ± 0.06
	11	96.0 ± 1.3	3.3 ± 1.1	0.8 ± 0.2
	30	93.9 ± 1.7	5.0 ± 1.4	1.1 ± 0.4
C145A	0.3	100	ND	ND
	11	99.8	0.2 ± 0.02	0.03 ± 0.01
	30	99.7 ± 0.1	0.2 ± 0.1	0.05 ± 0.02
Y174F	0.3	100	ND	ND
	11	100	ND	ND
	30	100	ND	ND
K178R	0.3	99.8 ± 0.1	0.2 ± 0.1	0.03 ± 0.02
	11	95.2 ± 1.7	4.1 ± 1.5	0.6 ± 0.02
	30	96.1 ± 1.3	3.3 ± 1.0	0.6 ± 0.2
K217A	0.3	100	ND	ND
	11	100	ND	ND
	30	99.7 ± 0.06	0.2 ± 0.05	0.04 ± 0.02
R306A	0.3	100	ND	ND
	11	89.0 ± 0.2	8.5 ± 0.1	2.4 ± 0.03
	30	80.1 ± 0.3	15.6 ± 0.2	4.3 ± 0.1

[a] M= GDP-α-D-mannose, Ga = GDP-β-L-galactose, Gu = GDP-β-L-gulose. ND indicates that the compound was not detected.

since these residues are part of the catalytic triad. The data suggest that K217 and C145 are important for the catalytic activity of the enzyme.

Discussion

Mechanism: Hydride Transfer. During hydride abstraction from the C4′ position of GDP-α-D-mannose, a proton is also removed from the O4′ hydroxyl of the sugar. In our structures of Y174, part of the catalytic triad is appropriately positioned to function as the base. The pK_a of tyrosine in SDR enzymes is known to be lowered by the positive charge of the catalytic triad lysine (K178 in GME).[5251−52] S143 hydrogen bonds to O4′, and we predict it fine-tunes the pK_a of the O4′ hydroxyl group; this is consistent with our other studies.[53] We see no evidence for a proton shuttle involving S143. In a study of RmlB with substrate bound, the importance of the relative positions of the C4 atoms of the carbohydrate and nicotinamide, for efficient hydride transfer, was noted.[49] In the GDP-α-D-mannose, GDP-β-L-gulose, and GDP-β-L-galactose structures, the nicotinamide C4 and carbohydrate C4′ are separated by an average of 3.9 Å. The hydrogen on the C4′ sugar ring points toward the nicotinamide. The structure of the GDP-β-L-4-keto-gulose intermediate places the C4′ atom 3.2 Å from the C4 of NADH and correctly oriented for its reduction to GDP-β-L-gulose. GME is able to bind and orient three distinct sugars such that each can participate in the hydride transfer at their C4′ positions. This degeneracy in recognition does not appear to result from a lack of hydrogen bonds to the sugar. The hydroxyl groups of each carbohydrate are recognized by direct hydrogen bonds to the protein (Figure 3d), nor does it appear to arise from conformation changes in protein or change in sugar position. We do not see any reaction with GDP-α-D-glucose; this is possibly a reflection of a very unfavorable equilibrium. Alternatively, it could suggest that the enzyme is not promiscuous and discriminates between two sugars which differ in the configuration of O2′. We prefer the latter explanation for two reasons. First, our HPLC assay can detect small amounts of sugar nucleotides; even a 99.5 to 0.5% equilibrium should be visible. Second, a model of GDP-α-D-glucose as substrate results in severe (<2.7 Å) steric clashes with the protein main chain at G104. This combination of versatility and selectivity is an interesting observation and is unusual for protein carbohydrate recognition.

Mechanism: Identification of the Acid and Base. The keto function lowers the pK_a of any proton α to it by stabilizing the carbanion formed by proton abstraction. GME must carry out the epimerization of C3′ and C5′ in sequence; it is not possible to abstract two protons simultaneously. The fact that we see only GDP-β-L-gulose and not GDP-D-altrose establishes that GME can epimerize C5′ first and C3′ second. It is possible that there is no obligate order of epimerization and that GME does epimerize C3′ first also. This would require that GDP-D-altrose is not released by the enzyme and always undergoes a second epimerization.

In both structures of GDP-D-mannose, only three residues, R306, S143, and C145, are within 4.0 Å of the C5′ atom (Figure 3d). R306 hydrogen bonds to the carbohydrate, and one would expect that it is fully protonated below pH 12. The angle between the NH1 atom of R306, the proton, and the C5′ atom of GDP-α-D-mannose varies between 120 and 130° and is not ideal for proton abstraction. S143 is part of the catalytic triad and will be a poor base (pK_a = 13) unless activated by acid residues, none of which are present here. Crucially, the angle between the OG atom of S143, the proton, and the C5′ atom of GDP-α-D-mannose varies between 90 and 100° and is thus inconsistent with proton abstraction. C145 has a much more amenable pK_a of 8.3, and its deprotonation during enzyme mechanisms is well precedented. The angle between the SG atom of C145, the proton, and the C5′ atom of GDP-α-D-mannose varies between 150 and 160°, close to the ideal of 180° for proton abstraction. R306 is 3.5 Å from the SG atom of C145, a positively charged R306 would stabilize the thiolate form of C145, lowering the pK_a. Structural data and chemical reasoning argue strongly for C145 as the base; the residue has no other obvious role in catalysis or substrate recognition. We assayed C145A, C145S, and R306A GME for activity (Table 2). C145A appears completely inactive, whereas R306A retains some activity, although significantly reduced. We interpret these data as supporting C145 as the base and that R306, although important, is not crucial. Interestingly, C145S shows very weak but measurable activity, suggesting that serine can to a very limited extent compensate for cysteine. This is consistent with the chemical similarities and differences between the two amino acids functioning as a base. Similar partial compensation of serine for cysteine was seen in two studies of amino acid racemases.[54,55] Comparison with other SDRs provides further support of C145 as base, in RmlB E136 is found in the same position. E136 has been confirmed as the base which abstracts the C5′ proton of dTDP-β-L-4-keto-glucose.[46] In GMER, C109 is found at this position, and this residue was identified as playing an important role in epimerization.[38] We observe a hydrogen bond between S143 and C145 in all of our structures.

(51) Wallace, A. C.; Laskowski, R. A.; Thornton, J. M. *Protein Eng.* **1995**, *8*, 127−134.
(52) Liu, Y.; Thoden, J. B.; Kim, J.; Berger, E.; Gulick, A. M.; Ruzicka, F. J.; Holden, H. M.; Frey, P. A. *Biochemistry* **1997**, *36*, 10675−10684.
(53) Blankenfeldt, W.; Kerr, I. D.; Giraud, M.-F.; McMiken, H. J.; Leonard, G.; Whitfield, C.; Messner, P.; Graninger, M.; Naismith, J. H. *Structure* **2002**, *10*, 773−786.
(54) Glavas, S.; Tanner, M. E. *Biochemistry* **1999**, *38*, 4106−4113.
(55) Koo, C. W.; Sutherland, A.; Vederas, J. C.; Blanchard, J. S. *J. Am. Chem. Soc.* **2000**, *122*, 6122−6123.

Scheme 3. R = OGDP Proposed Mechanism. Shown Boxed Is the Central Keto Sugar Intermediate Found in the K178R Mutant Crystal Structure

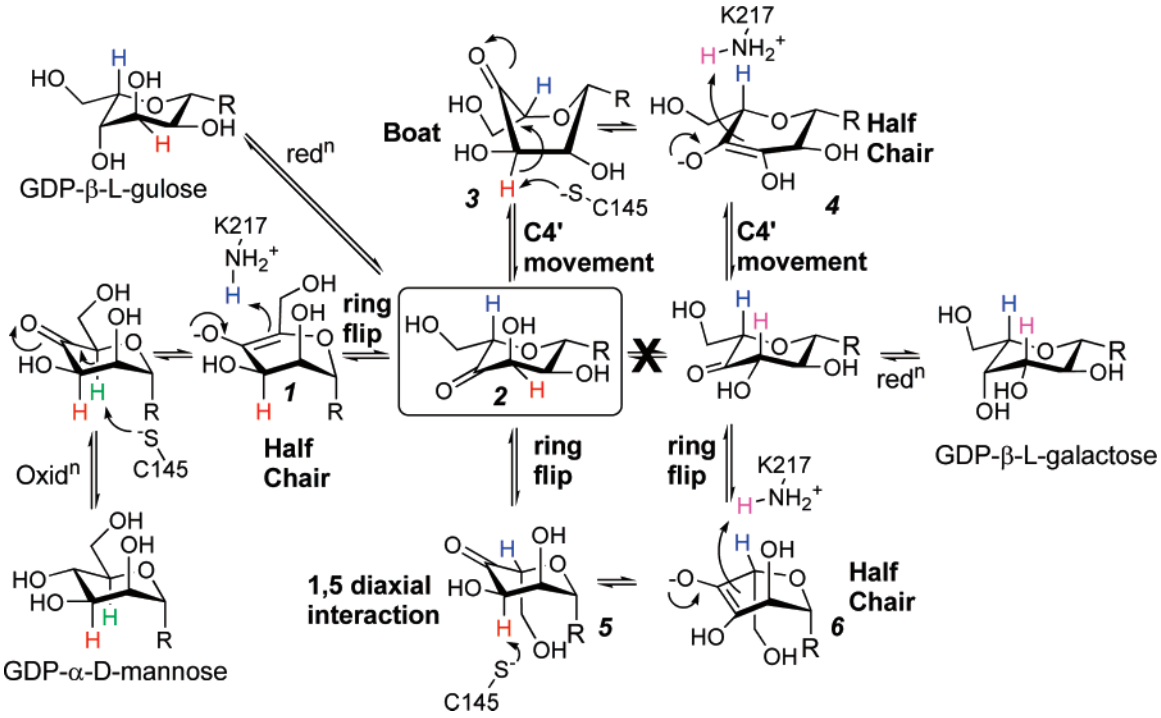

Others have suggested a role for serine in adjusting the pK_a of cysteine.[38] The removal of the proton from GDP-α-D-mannose creates an enolate, and in GME, the enolate would be hydrogen bonded to Y174 and S143. These hydrogen bonds would stabilize the enolate.

Epimerization requires addition of a proton to the opposite sugar face from that of C145. After examination of the co-complexes, the only chemically reasonable candidate is K217. In one of its conformations, the NZ atom is appropriately positioned to act as the acid for C5′. We investigated the role of this residue by making a K217A mutation. This mutant was inactive, supporting our assignment of this residue as the second catalytic acid/base. The structure confirms that the mutant does not substantially perturb the protein. The mechanism would require that the pK_a of K217 is lower than that of free lysine (10.8). Lowering of the pK_a of lysine can be accomplished by location in an apolar environment. In the "active" conformation of the K217, the NZ atom makes only one hydrogen bond. In GMER, site-directed mutagenesis identified H179, which superimposes upon K217, as an important residue in epimerization.[38]

Interestingly, all the active mutations preserve the ratio between GDP-β-L-gulose and GDP-β-L-galactose despite not reaching equilibrium. In no case do we see appearance of GDP-D-altrose, suggesting that the mutants equally perturb C5′ and C3′ epimerization. Repeating the analysis detailed above for the C3′ position, we identify the same two residues, C145 and K217, as the key acid/base pair. To carry out the second epimerization, the protonation state has to be reset. Whether this is done by partial or complete release of GDP-β-L-gulose or some hydrogen bond network involving the many waters at the active site is not known.

Mechanism: Carbohydrate Conformation. Epimerization of the C5′ position is conventionally written showing the equatorial group moving from an equatorial position to an axial one, followed by a ring flip (Scheme 1). Structural analysis suggests that an axial orientation of C6′−O6′ is unlikely to occur. O6′ occupies the same position in substrate, product, and intermediate (Figure 3b and c). An axial orientation of the C6′−O6′ group would clash with R306 and C145 on one face and the main chain at N203 on the other. Deformation of the protein is possible, but there is no evidence that such flexibility exists in GME. Movement of C6′−O6′ requires the breaking of two protein to sugar hydrogen bonds. An alternative proposal is that the ring flip occurs as the proton is being transferred to the half-chair carbanion (compound **1** in Scheme 3). The location of C6′−O6′ remains fixed with the other atoms of the ring adjusting their position to achieve a ring flip during proton transfer. In this mechanism, the proton is transferred directly to the axial position rather than an equatorial one, which then ring flips to an axial position. The abstraction from and donation to an axial position is favored.

The second epimerization (conversion of GDP-β-L-gulose to GDP-β-L-galactose) requires that the proton is removed from C3′. In light of the structural data, there is a difficulty with this process as conventionally written. In GDP-β-L-gulose (and the keto sugar), the C3′ proton is equatorial and the O3′ atom is axial (compound **2** in Scheme 3). This places the proton in the incorrect orientation for removal by C145. More seriously, an equatorial proton has a significantly higher pK_a than an axial one.[56] Lowering of the pK_a of an α proton requires a trans arrangement of the π^* antibonding orbital of the keto group and σ bonding orbital of the α CH. In ring structures, this requires that the CH group is axial. The principle of microscopic reversibility dictates that proton addition also requires a similar orientation of the keto group and α proton. There are two distortions of GDP-β-L-4-keto-gulose which give the correct orientation of the CH group relative to the keto group; first,

(56) Corey, E. J. *J. Am. Chem. Soc.* **1954**, *76*, 175−179.

the sugar may ring flip into the alternate chair form (compound **5** in Scheme 3). This would place the C3′ proton in an axial position but would also place C6′−O6′ in an axial position, which seems unlikely from our structural data. The ring-flipped conformation of GDP-*β*-L-gulose would be significantly strained by a 1,5 diaxial clash between C6′−O6′ and O1′. The second epimerization reaction would operate on a very high energy intermediate, and the transition state would have some 1,3,5 triaxial character, which is extremely unfavorable (compound **6** in Scheme 3). All this would present a formidable kinetic barrier to the second epimerization. We see no evidence for an initial accumulation of GDP-*β*-L-gulose in the mutants, suggesting the second epimerization is not significantly slower than the first. The alternative to a complete ring flip is for GDP-*β*-L-4-keto-gulose to adopt a boat structure (compound **3** in Scheme 3). This is achieved by the C4′ atom moving through the plane of the ring (Scheme 3). This results in the proton at C3′ being axial relative to the keto group. Although boats are high in energy, they have been observed in several protein carbohydrate complexes.[57] They are found in "skew" conformation rather than a perfect geometric boat.[57] The presence of a keto group at C4′ reduces the strain required to form a boat by decreasing the 1,4 interaction. A skew boat structure has the advantage that it avoids the 1,5 diaxial interaction, leaves C6′−O6′ unchanged, and its transition state avoids any 1,3,5 triaxial character (compound **4** in Scheme 3). Robustly distinguishing between the ring flip and skew boat routes experimentally is all but impossible for this enzyme, and the level of calculations required to be convincing are beyond the scope of this paper.

Implications for Other Carbohydrate Epimerases. The studies here provide important insight into the mechanism of GMER. Although no co-complex has ever been reported for GMER, a series of site-directed mutants and mutant crystal structures have been reported. GMER, like GME, requires an acid and a base for each of the epimerization reactions. Superimposing GMER upon our co-complexes strongly supports C109 and H178 as the acid/base pair in GMER. The cysteine side chains are oriented identically in both enzymes, making the same hydrogen bonds. S107 in GMER fulfills exactly the same role as S143 in GME. Stabilization of the thiolate in GME is provided by R306 and in GMER K283 could fulfill the same role. As well as main chain superposition of the two residues, the imidazole ring of H178 in GMER occupies the same space as the lysine side chain of K217 in GME. In the GMER study, H178 and C109 were both mutated to alanine, resulting in complete loss of epimerization.[38] The order of epimerization in GMER has never been addressed, and no intermediate compounds have been reported. Irrespective of the order of epimerization in GMER, the second epimerization in GMER presents the same problem as in GME. Either the second epimerization creates a highly strained 1,5 (or 1,3) diaxial intermediate or it goes through a twist. The observation that a single acid/base pair is responsible for two epimerizations is relevant to the RmlC class of enzyme.[58] These enzymes only epimerize the positions α to the keto group of dTDP-4-keto-6-deoxy-glucose; they have no redox chemistry and have a different structure to GME (or GMER). In RmlC, a single acid/base pair was also proposed to be responsible for both epimerizations.[59] The deduction that in GME the single C5′ epimerized product undergoes ring flip during proton transfer seems likely to be true for the very closely related intermediate in RmlC. The enzyme ADP-L-glycero-D-manno-heptose 6-epimerase (AGME) inverts the chirality at C6′. Like GalE, epimerization is a result of transient keto formation at the inverted carbon.[60] Unlike GalE, there is no large rotation of the carbohydrate, instead just the C6′ group rotates. This requires an acid/base pair, while one is probably Y140 (of the AGME catalytic triad) the other residue is not known.[61] The main chain of K178 of AGME[62] does not superimpose with K217 of GME; however, the NZ atoms in the superimposed structures are close in space, suggesting K178 is the other acid base residue in AGME.

Conclusions

GME is an unusual enzyme from several standpoints. It carries out three chemical reactions and acts on three different carbohydrates, yet still preserves substrate selectivity. It is able to accomplish two epimerizations using the same acid/base pair of residues. The location of this acid/base pair appears to be conserved in several other SDR enzymes. We have determined the first structure of a two-site carbohydrate epimerase bound to its substrate, product, and monoepimerized intermediate. We have also trapped the key keto sugar intermediate at the active site. The high resolution of the structural studies has made it possible to determine the conformation of intermediates, helping to delineate the mechanistic possibilities of GME.

Experimental Procedures

Cloning, Mutagenesis and Protein Purification. The gene for *A. thaliana* GDP-mannose-3′,5′-epimerase was subcloned from pDONR201-GME[20] using PCR amplification of the gene; the restriction sites *Nde* I and *Sac* I were introduced in the F and R primers, respectively (GME_F: GGCTCCAUCCATGGUGAACTAC; GME_R: GAAAGCUGAGCTCUTCACTCTTTTC; restriction sites are underlined). After amplification, the PCR product was digested with *Nde* I and *Sac* I restriction enzymes and cloned into the pEHISTEV vector (an engineered variant of pET30 with an N-terminal 6x His tag that is cleaved by Tobacco Etch Virus (TEV) protease) (Dr H. Liu, personal communication) digested with the same restriction enzymes. The construct was confirmed by DNA sequencing performed by The Sequencing Service (School of Life Sciences, University of Dunedee, Scotland, www.dnaseq.co.uk) using Applied Biosystems Big-Dye Ver 3.1 chemistry on an Applied Biosystems model 3730 automated capillary DNA sequencer. Active-site mutants of GME were constructed in the pEHISTEV-GME vector using the Qiagen QuikChange Site-Directed Mutagenesis Kit according to manufacturer's instructions. The primers used for this mutagenesis are listed in Table 3. No mutant has a single base pair change at the third nucleotide position.

E. coli Rosetta (DE3) cells (Novagen) transformed with pEHISTEV-GME (mutant and wt) were grown on Luria-Bertani (LB) agar plates containing kanamycin (50 $\mu g \cdot mL^{-1}$) at 37 °C for 16 h. A single colony was used to inoculate 100 mL of LB medium containing 50 $\mu g \cdot mL^{-1}$ kanamycin; this was incubated at 37 °C for 16 h with shaking; 10 mL

(57) Vasella, A.; Davies, G. J.; Matthias, B. *Trends Chem. Biol.* **2002**, *6*, 619−629.
(58) Giraud, M.-F.; Leonard, G. A.; Field, R. A.; Berlind, C.; Naismith, J. H. *Nat. Struct. Biol.* **2000**, *7*, 398−402.
(59) Dong, C.; Major, L. L.; Allen, A.; Blankenfeldt, W.; Maskell, D.; Naismith, J. H. *Structure* **2003**, *11*, 715−723.
(60) Read, J. A.; Ahmed, R. A.; Morrison, J. P.; Coleman, W. G., Jr.; Tanner, M. E. *J. Am. Chem. Soc.* **2004**, *126*, 8878−8879.
(61) Morrison, J. P.; Read, J. A.; Coleman, W. G., Jr.; Tanner, M. E. *Biochemistry* **2005**, *44*, 5907−5915.
(62) Deacon, A. M.; Ni, Y. S.; Coleman, W. G., Jr.; Ealick, S. E. *Structure* **2000**, *8*, 453.

Table 3. Primers for GME QuikChange Mutagenesis

Oligo	mutation	sequence (5′-3′) (site of mutation in bold)
C145A_F	C145A	CTTTTATGCTTCGAGTGCT**GCT**ATCTATCCAGAGTTTAAGC
C145A_R		GCTTAAACTCTGGATAGAT**AGC**AGCACTCGAAGCATAAAAG
C145S_F	C145S	TTTATGCTTCGAGTGCT**TCT**ATCTATCCAGAGTTTAAGC
C145S_R		GCTTAAACTCTGGATAGAT**AGA**AGCACTCGAAGCATAAA
Y174F_F	Y174F	GAGCCTCAAGATGCT**TTT**GGTTTGGAGAAGCTTGC
Y174F_R		GCAAGCTTCTCCAAACC**AAA**AGCATCTTGAGGCTC
K178R_F	K178R	GCTTATGGTTTGGAG**AGG**CTTGCTACGGAGGA
K178R_R		CTCCTCCGTAGCAAG**CCT**CTCCAAACCATAAGC
K217A_F	K217A	GGTGGAAGGGAG**GCG**GCTCCAGCTGC
K217A_R		GCAGCTGGAGC**CGC**CTCCCTTCCACC
R306A_F	R306A	GGAAGGTGTTCGTGGT**GCT**AACTCAGACAACAATC
R306A_R		GATTGTTGTCTGAGTT**AGC**ACCACGAACACCTTCC

of culture was used to inoculate 1 L of LB medium containing 50 mg·L^{-1} kanamycin, and cells were grown with shaking (200 rpm) at 37 °C. When $OD_{600} = 0.5$, the temperature was dropped to 24 °C and protein expression induced with 0.1 mM IPTG, and the cells were grown overnight. Cells were harvested by centrifugation (7 krpm, 10 min, 4 °C), and the pellet was stored at −80 °C. Pellets were resuspended in lysis buffer (PBS, 300 mM NaCl, 10 mM imidazole, 1 mM DTT, 1 mini complete EDTA-free protease inhibitor tablet (Roche) per 10 mL buffer). Cells were lysed by sonication, and the sample was centrifuged for 30 min at 20000 rpm at 4 °C and cell debris discarded. Supernatant was filtered through a 0.2 μm filter and loaded on a Ni^{2+}-NTA agarose column. His-tagged GME was eluted with a solution of PBS, 300 mM NaCl, and 100 mM imidazole. The protein was dialyzed into TEV cleavage buffer (PBS, 50 mM Tris pH 7.5, 300 mM imidazole, 0.5 mM EDTA, 2 mM DTT) and digested overnight with TEV protease. GME was dialyzed into 20 mM Tris pH 7.5, 50 mM NaCl, and further purified on a Ni^{2+}-NTA agarose column, followed by size exclusion on a Sephacryl S-200 column. After gel filtration, 1 mM DTT was added to the protein, which was concentrated to around 4.5 mg·mL^{-1} using Millipore regenerated cellulose 10 kDa membranes in an Amicon 8200 concentrator. SeMet GME protein was prepared by essentially the same method as native, except cells were grown in a SeMet containing minimal media.[63] SeMet incorporation was confirmed by mass spectrometry.

Crystallography. Crystallization was performed by a sitting drop vapor diffusion method at 21 °C using 4 mg·mL^{-1} protein and drops with a 1:1 ratio of protein:mother liquor. Crystals for diffraction were obtained from a mother liquor of 2.2 M $(NH_4)_2SO_4$, with either 100 mM Hepes (pH 7.0−7.75) or 100 mM BisTris (pH 5.5−7.0). Cocrystals with GDP-D-mannose or GDP-L-galactose were obtained by incubating the protein with 2 mM nucleotide−sugar prior to crystallization. All crystals were isomorphous with space group $P2_1$ and cell constants of $a = 62.8$ Å, $b = 83.8$ Å, $c = 66.2$ Å, and $\beta = 98.9°$ (Table 1). MAD data from a selenomethionine-labeled crystal of GME-K178R were collected on BM14 UK ($\lambda_{peak} = 0.979$, $\lambda_{remote} = 0.886$) of the European Synchrotron Radiation Facility (ESRF) at Grenoble, France. Other data sets were collected on ESRF ID14-1 (GME-K178R, $\lambda = 0.934$; GME-Y174F GDP-L-galactose complex, $\lambda = 0.933$; and GME-Y174F GDP-D-mannose complex, $\lambda = 0.933$) and in house (wild-type GME; $\lambda = 1.542$). All crystals were collected at 100 K after first soaking in 6 M sodium formate. Data were indexed and integrated in MOSFLM, version 6.2.5[64] and scaled in SCALA version 3.2.5.[65] Initial phases were determined experimentally using SOLVE[66] and improved with RESOLVE.[67,68] Phases were extended to 2 Å using DM.[69] ARPwARP[70] and manual intervention in O[71] gave a complete model to 1.5 Å. The model was refined with Refmac 5.2.0016,[72] and water molecules were added using ARPwARP; 5% of experimental structure factors were excluded for R_{free} calculation. All other structures were solved by molecular replacement (using K178R) and refined in the same way. The same set of indices were omitted for all R_{free} calculations. Structural homologues were determined using the Dali server[73] (http://www.ebi.ac.uk/dali/); pairwise structural comparisons were then made for the top four hits using DaliLite[74] (http://www.ebi.ac.uk/DaliLite/). Molecular representations were prepared with Pymol.[75]

GME Assay. Enzymatic activity of wild-type, C145S, C145A, Y174F, K178R, K217A, and R306A GME enzymes was detected by monitoring the presence of GDP-α-D-mannose, GDP-β-L-galactose, and GDP-β-L-gulose. Assays contained 0.3, 11, or 30 μM enzyme, 150 μM GDP-α-D-mannose, 50 mM Tris pH 8.0, and were performed in triplicate. Reaction mixtures were incubated overnight at 21 °C, protein was removed from the mixtures by centrifugation through an amicon microcon 10 kDa molecular cutoff regenerated cellulose column prior to being loaded onto a Varian OmniSpher C-18 column (250 × 4.6 mm) at a flow rate of 1 mL·min^{-1}. The column was previously equilibrated with 20 mM triethylammonium acetate (TEAA), pH 6.0. After isocratic elution with 20 mM TEAA pH 6.0 for 7 min, nucleotide sugars eluted during a linear gradient of 0−1% acetonitrile in 20 mM TEAA, pH 6.0, over 28 min. NAD^+ eluted with a linear gradient of 1−25% acetonitrile in 20 mM TEAA pH 6.0 over 10 min. This method is based on that of Järvinen et al.[76] Eluant was monitored by a UV detector at 254 nm. NAD^+, GDP-α-D-mannose, GDP-β-L-gulose, and GDP-β-L-galactose were identified by coelution with authentic standards. The peaks from the assay were also characterized by mass spectrometry and confirmed to have the correct molecular weight. Authentic GDP-α-D-mannose was purchased from SIGMA; GDP-β-L-gulose was obtained from crystals of K178R GME, and GDP-β-L-galactose was a gift. For isolation of GDP-β-L-gulose from K178R GME crystals, the crystals were dissolved/denatured in 500 μL of 50% v/v acetonitrile, and protein was removed by centrifugation. Supernatant was dried in a vacuum centrifuge and resuspended in 1.5 mL of 5 mM NH_4HCO_3. GDP-β-L-gulose was purified on CarboPrep 90 columns (Restek) using the method of Räbinä et al.[77] After elution samples were dried by vacuum centrifugation and resuspended in 10 mM Tris pH 8.0, HPLC analysis shows one major peak with a correct mass of 604

(63) Van Duyne, G. D.; Standaert, R. F.; Karplus, P. A.; Schreiber, S. L.; Clardy, J. *J. Mol. Biol.* **1993**, *229*, 105−124.
(64) Leslie, A. G. W. *Joint CCP4 and ESF-EAMCB Newsletter on Protein Crystallography* **1992**, *26*, 1−10.
(65) Evans, P. R. *Joint CCP4 and ESF-EACBM Newsletter* **1997**, *33*, 22−24.
(66) Terwilliger, T. C.; Berendzen, J. *Acta Crystallogr., Sect. D* **1999**, *D55*, 849−861.
(67) Terwilliger, T. C. *Acta Crystallogr., Sect. D* **2000**, *D59*, 34−44.
(68) Terwilliger, T. C. *Acta Crystallogr., Sect. D* **2002**, *D59*, 34−44.
(69) Cowtan, K. *Joint CCP4 and ESF-EACBM Newsletter on Protein Crystallography* **1994**, *31*, 34−38.
(70) Perrakis, A.; Morris, R.; Lamzin, V. S. *Nat. Struct. Biol.* **1999**, *6*, 458−463.
(71) Jones, T. A.; Zou, J. Y.; Cowan, S. W.; Kjeldgaard, M. *Acta Crystallogr., Sect. A* **1991**, *47*, 110−119.
(72) Murshudov, G.; Vagin, A. A.; Dodson, E. J. *Acta Crystallogr., Sect. D* **1997**, *53*, 240−255.
(73) Holm, L.; Sander, C. *Proteins* **1994**, *19*, 165−173.
(74) Holm, L.; Park, J. *Bioinformatics* **2000**, *16*, 566−567.
(75) DeLano, W. L. DeLano Scientific, San Carlos, CA, USA **2002**.
(76) Järvinen, N.; Mäki, M.; Räbinä, J.; Roos, C.; Mattila, P.; Renkonen, R. *Eur. J. Biochem.* **2001**, *268*, 6458−6464.
(77) Räbinä, J.; Mäki, M.; Savilahti, E. M.; Järvinen, N.; Penttilä, L.; Renkonen, R. *Glycoconjugate J.* **2001**, *18*, 799−805.

and two minor peaks that coelute with GDP-β-D-mannose and GDP-β-L-galactose.

Acknowledgment. GDP-β-L-galactose was a generous gift from Prof. Joachim Thiem, Institute for Organic Chemistry, University of Hamburg. Garib Murshudov provided invaluable assistance with refmac refinement of linked compounds. We thank Martin Tanner for help with Scheme 3. The work is supported by a Wellcome Trust Program Grant. The use of Biotechnology and Biological Science Research Council (BBSRC) and Scottish Higher Education Funding Council structural proteomics facilities is acknowledged. J.H.N. is a BBSRC career development fellow. We acknowledge the use of BM14UK and other ESRF beamlines.

Supporting Information Available: Stereodiagrams of ligand density; initial (Figure S1) and final (Figure S2) refinement of K178R GME GDP-sugar density; unbiased NAD^+ density from K178R GME (Figure S3); initial (Figure S4) and final (Figure S5) refinement of NAD^+ density from K178R GME; unbiased GDP-sugar density for K178R GME (Figure S6), wild-yype GME (Figure S7), GDP-α-D-mannose from K217A GME (Figure S8), and GDP-β-L-galactose from Y174F GME (Figure S9). Stereodiagrams of overlayed NAD^+ molecules (Figure S10) and GDP-sugar molecules from all eight subunits (Figures S11 and S12). A stereodiagram of K217 density from Y174F GME. HPLC traces from reactions with wild-type and mutant GME enzymes. A table of rmsd values between A subunit core regions of the four different GME structures. This material is available free of charge via the Internet at http://pubs.acs.org.

JA056490I